

Fracture, fatigue, and creep of nanotwinned metals

Xiaoyan Li, Ming Dao, Christoph Eberl, Andrea Maria Hodge, and Huajian Gao

As a relatively new class of hierarchically structured materials, nanotwinned (NT) metals exhibit an exceptional combination of high strength, good ductility, large fracture toughness, remarkable fatigue resistance, and creep stability. This article reviews current studies on fracture, fatigue, and creep of NT metals, with an emphasis on the fundamental deformation and failure mechanisms. We focus on the complex interactions among cracks, dislocations, and twin boundaries, the influence of microstructure, twin size, and twinning/detwinning on damage evolution, and the contribution of nanoscale twins to fatigue and creep under indentation and irradiation conditions. The article also includes critical discussions on the effects of twin thickness and grain size on the fracture toughness, fatigue resistance, and creep stability of NT metals.

Introduction

Over the past decade, the fabrication of nanotwinned (NT) metals with ultrahigh strength and good ductility has been recognized as a remarkable breakthrough in the area of metallic structured materials. These materials exhibit a hierarchical microstructure, with a large number of highly organized nanoscale twins embedded within micron- or submicron-sized grains^{1,2} (Figure 1).

Twin boundaries (TBs) with low energy and high symmetry not only act as obstacles to dislocation motion, but they also store a high density of mobile dislocations, leading to macroscopic hardening and strengthening, as well as improved ductility of NT materials compared to their nanocrystalline counterparts.^{2,3} Experimental studies^{1,2,4–14} have shown that NT metals possess excellent mechanical properties, such as ultrahigh strength, good ductility, large fracture toughness, remarkable fatigue resistance, and creep stability. Fabrication methods for NT metals include electrodeposition,^{1,2} physical vapor deposition (e.g., magnetron sputtering)^{5,6} and dynamic plastic deformation (DPD) (a synthesis technique for bulk nanostructured metals based on plastic deformation at high strain rates or low temperatures).^{10,11} The characteristic length scale of the twin structures produced from deposition methods can be tuned to below 10 nm.

Figure 1a–b shows typical transmission electron microscope (TEM) images of electrodeposited NT Cu with equiaxed grains¹ and magnetron sputtered epitaxial Ag with columnar grains,² respectively. The twin structures produced by DPD are deformation twins that are emitted from grain boundaries (GBs) or free surfaces during severe plastic deformation. Figure 1c shows TEM images of a three-order twinned structure in a twinning-induced plasticity (TWIP) steel sample via surface mechanical attrition treatment.¹⁵ It is also interesting that a gradient NT structure can be generated by subjecting a TWIP steel bar to torsion.¹⁶ For more details and discussions of growth and deformation twins in NT metals, see the review article by Beyerlein et al.¹⁷ and viewpoint paper by Mahajan.¹⁸ Plenty of experimental, computational, and theoretical studies^{1,2,4–16,19–33} have been conducted to investigate the mechanisms of plastic deformation in NT metals (e.g., interactions between TBs and dislocations) and related size effects (e.g., the influence of TB spacing on the strength and ductility of materials). Some of the recent advances in this area have been reviewed in the literature.^{34,35}

Understanding the damage tolerance (such as fracture and fatigue resistance) and time-dependent deformation behaviors (such as creep stability) of NT metals are essential for

Xiaoyan Li, Centre for Advanced Mechanics and Materials, Applied Mechanics Laboratory, Department of Engineering Mechanics, Tsinghua University, China; xiaoyanlithu@tsinghua.edu.cn

Ming Dao, Department of Materials Science and Engineering, Massachusetts Institute of Technology, USA; mingdao@mit.edu

Christoph Eberl, Laboratory for Micro- and Materials Mechanics, Institute for Microsystems Technology, University of Freiburg, and Fraunhofer Institute for Mechanics of Materials, Germany;

chris.eberl@imtek.de and chris.eberl@iwm.fraunhofer.de

Andrea Maria Hodge, Mork Family Department of Chemical Engineering and Materials Science, University of Southern California, USA; ahodge@usc.edu

Huajian Gao, School of Engineering, Brown University, USA; huajian_gao@brown.edu

DOI: 10.1557/mrs.2016.65

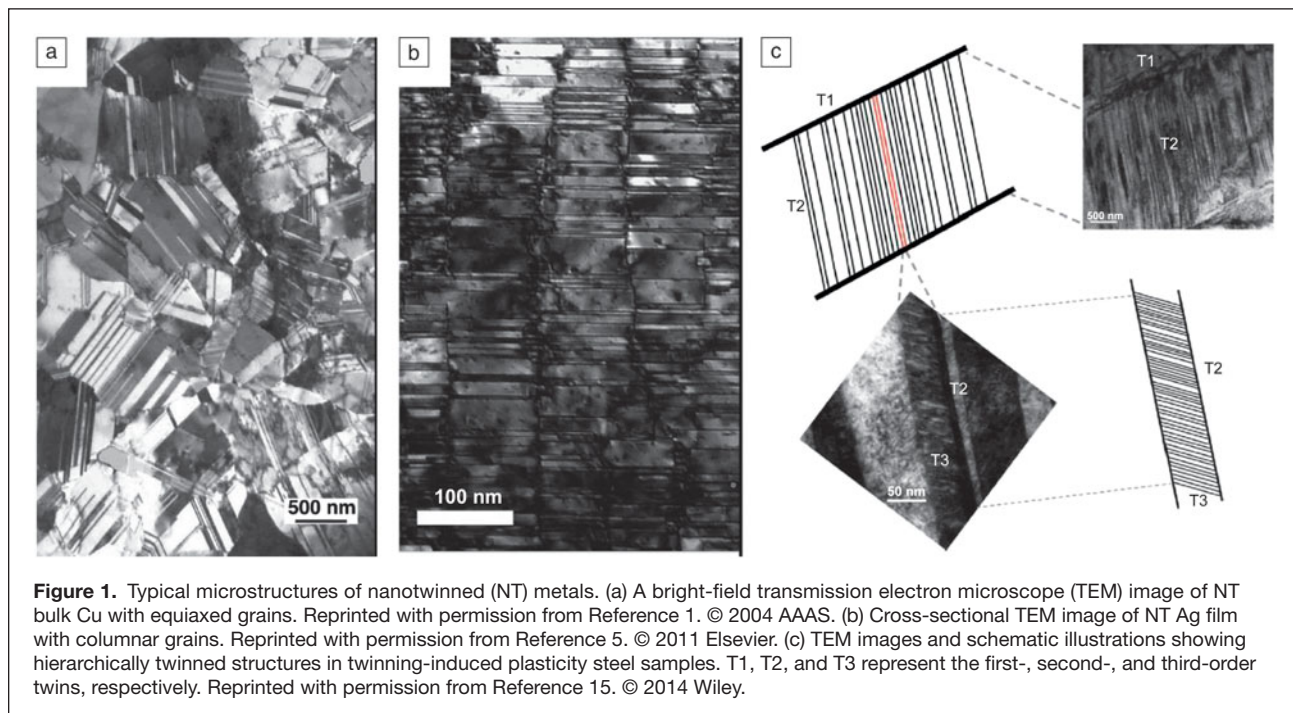


Figure 1. Typical microstructures of nanotwinned (NT) metals. (a) A bright-field transmission electron microscope (TEM) image of NT bulk Cu with equiaxed grains. Reprinted with permission from Reference 1. © 2004 AAAS. (b) Cross-sectional TEM image of NT Ag film with columnar grains. Reprinted with permission from Reference 5. © 2011 Elsevier. (c) TEM images and schematic illustrations showing hierarchically twinned structures in twinning-induced plasticity steel samples. T1, T2, and T3 represent the first-, second-, and third-order twins, respectively. Reprinted with permission from Reference 15. © 2014 Wiley.

their practical applications in structural materials and micro-/nanodevices. To date, a large amount of effort has been dedicated to exploring plastic deformation in NT metals, but there have also been an increasing number of studies on their failure and time-dependent behaviors, in spite of the experimental difficulties of precisely performing the fracture/fatigue/creep testing at the micro-/nanoscales and validly extracting the relevant material properties from the results of small specimens. In this article, we review recent advances in experimental, theoretical, and computational studies of the fracture, fatigue, and creep responses of NT metals. Here, we provide a critical discussion of the influence of twin size on fracture toughness, fatigue resistance, and creep stability. The objectives are to discuss the underlying failure mechanisms and to highlight opportunities for further research.

Fracture of nanotwinned metals

Fracture is a common failure mode in nanostructured materials with ultrahigh strength. However, to date, there have been few reports on the fracture of NT metals. Here, we first present unique fracture behaviors related to coherent TBs (CTBs). Next, we review recent studies of the fracture of various NT specimens in bulk, thin-film, and nanopillar/nanowire forms or with hierarchically twinned structures. Finally, we introduce recent reports of the interaction between cracks and TBs.

In contrast to general GBs, CTBs exhibit remarkably unusual fracture behaviors due to their low energy and high symmetry. When an atomistically sharp crack lies on a $\{111\}$ CTB, it cleaves in one of the $\langle 112 \rangle$ directions along the TB,

indicating the intrinsic brittleness of TBs. However, the crack emits dislocations when propagating in the opposite direction. This directional anisotropy in brittle-ductile responses (**Figure 2a**) of CTBs has been demonstrated by atomistic simulations and theoretical analyses.³⁶ A recent experimental study³⁷ on the hydrogen-assisted fracture of a Ni-based superalloy showed that a CTB is more susceptible to crack initiation than general GBs in a hydrogen environment. This is thought to originate from enhanced dislocation activity along the CTB.

Qin et al.^{10,11} measured the fracture toughness of NT bulk Cu (with TB spacing $\lambda = 40\text{--}50$ nm) prepared by DPD using three-point bending tests, and found that the fracture toughness increases with an increase in the volume fraction of nanoscale twins. They also observed three types of dimples on the fracture surface: (1) fine/shallow dimples with an average size of $4\text{--}6$ μm (dashed circle in Figure 2b), (2) equiaxed dimples with a size of tens of micrometers, and (3) coarse/deep dimples with an elongated core at the bottom (solid circles in Figure 2b). The size of fine/shallow dimples is several times larger than the mean grain size of the specimen, similar to what is observed for nanocrystalline metals. However, the coarse/deep dimple is an unusual fracture characteristic in NT metals, and it is not observed in the fracture of nanocrystalline metals. Its formation is due to the presence of highly anisotropic NT bundles. The enhanced fracture toughness is primarily attributed to the formation of coarse/deep dimples. Singh et al.¹² observed increased fracture toughness with decreasing average TB spacing using two electrodeposited NT Cu specimens with equiaxed grains (with the same mean grain size $d = 400\text{--}500$ nm, but $\lambda = 32\text{--}85$ nm), which is a different size

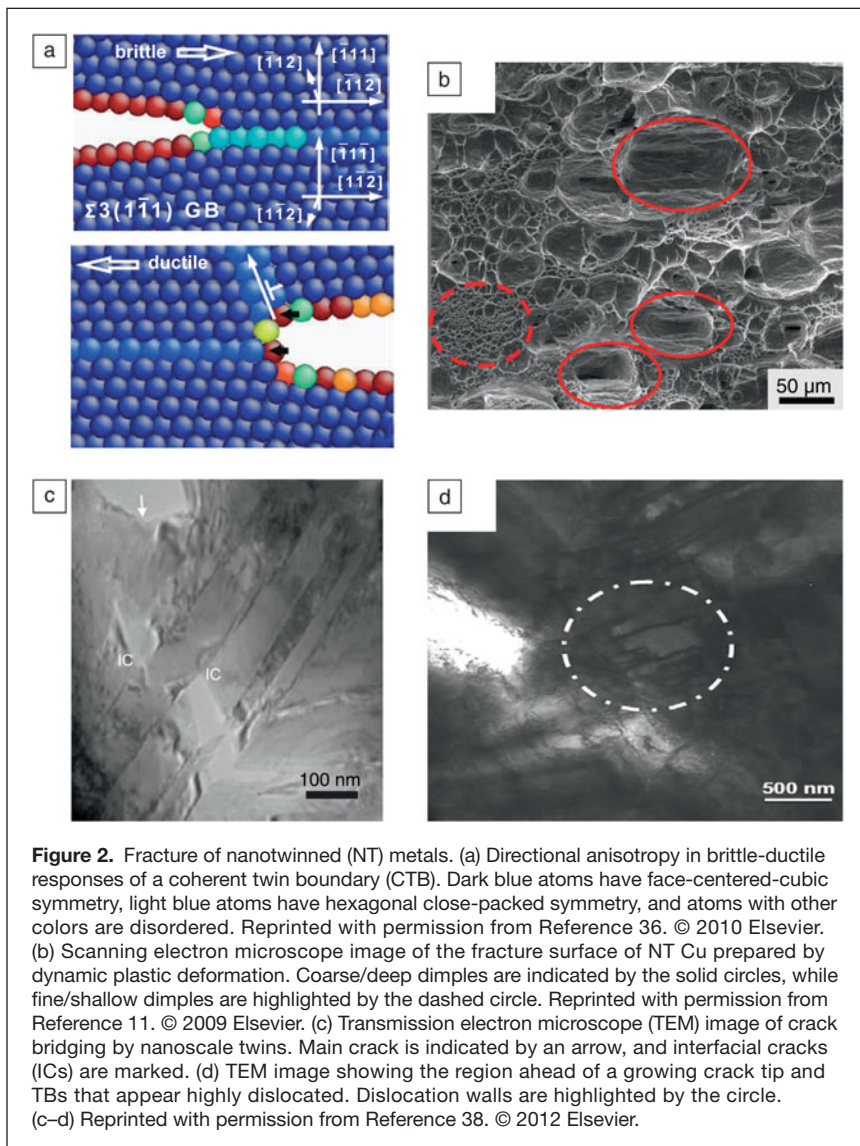


Figure 2. Fracture of nanotwinned (NT) metals. (a) Directional anisotropy in brittle-ductile responses of a coherent twin boundary (CTB). Dark blue atoms have face-centered-cubic symmetry, light blue atoms have hexagonal close-packed symmetry, and atoms with other colors are disordered. Reprinted with permission from Reference 36. © 2010 Elsevier. (b) Scanning electron microscope image of the fracture surface of NT Cu prepared by dynamic plastic deformation. Coarse/deep dimples are indicated by the solid circles, while fine/shallow dimples are highlighted by the dashed circle. Reprinted with permission from Reference 11. © 2009 Elsevier. (c) Transmission electron microscope (TEM) image of crack bridging by nanoscale twins. Main crack is indicated by an arrow, and interfacial cracks (ICs) are marked. (d) TEM image showing the region ahead of a growing crack tip and TBs that appear highly dislocated. Dislocation walls are highlighted by the circle. (c–d) Reprinted with permission from Reference 38. © 2012 Elsevier.

dependence as observed in nanocrystalline metals.³ They also pointed out the important influence of the plastic anisotropy of nanoscale twins.

Kim et al.³⁸ performed *in situ* TEM tensile testing on ultrafine-grained (UFG) Cu thin films with nanoscale twins and a thickness of ~ 100 nm. They observed a nanoscale toughening mechanism whereby the crack is arrested by TBs and nanoscale twins serve as crack-bridging ligaments (Figure 2c).³⁸ Kim et al.³⁸ also performed relevant atomistic simulations that showed a large number of dislocations emitted from a crack interacted with TBs ahead of the crack tip, transforming clean CTBs into impenetrable dislocation walls. These dislocation walls can strongly resist crack propagation, leading to crack arrest and bridging. The transformation from TBs to dislocation walls is evidenced by the TEM image shown in Figure 2d.

Although this experimental study³⁸ was conducted on thin-film samples, it reveals two important toughening mechanisms

that might be operative in NT bulk samples. Specifically, crack bridging due to nanoscale twins might provide an explanation of the formation of coarse/deep dimples in NT bulk samples. Shan et al.³⁹ conducted *in situ* TEM tensile experiments that showed the crack was deflected by TBs, resulting in a zigzag crack path when the thickness of the NT metal thin film was reduced to tens of nanometers. Recent molecular dynamics (MD) simulations⁴⁰ indicated that such zigzag cracking is due to screw dislocation-mediated local thinning ahead of the crack. Kobler et al.⁴¹ recently conducted *in situ* TEM tensile testing on a columnar-grained NT Cu thin film (with $\lambda = \sim 9$ nm). They observed orientation-dependent fracture/deformation behaviors whereby when the tensile direction was parallel to the TBs, fracture occurred along the original CTBs and incoherent TBs (ITBs) formed during deformation; when the tensile direction was perpendicular to the TBs, plastic deformation was accommodated by detwinning and the formation of new grains.

Jang et al.⁹ synthesized NT Cu nanopillars with diameters of 50–250 nm and $\lambda = 0.6$ –4.3 nm and they performed *in situ* TEM tension tests on these specimens. They found that when the tensile direction was perpendicular to the TBs, the specimen failed due to cleavage fracture (a brittle fracture mode in which the cross section of the specimen remains unchanged at fracture) if $\lambda > 3$ –4 nm; otherwise, the specimen failed due to necking, showing a significant reduction of the cross-section area prior to final fracture. They also performed MD simulations for Mode I crack propagation in quasi-

3D samples (i.e., samples with a periodic boundary imposed in the thickness direction, and the thicknesses is usually much smaller than the other two dimensions) to reveal the mechanism behind this brittle-to-ductile transition.⁹ The simulation results showed that when TB spacing was larger than a critical value, cleavage occurred along a TB due to the intrinsic brittleness of the TBs;³⁶ otherwise, the stress field around the crack-tip induced dislocation nucleation on a neighboring TB, eventually giving rise to ductile fracture of the sample. Jang et al.⁹ developed a theoretical model, based on the important insights from experiments and simulations, to predict the critical TB spacing for the brittle-to-ductile transition, with predictions consistent with experimental and simulation results.

Wang et al.⁴² conducted *in situ* TEM tension tests on NT Au nanowires with diameters of 8–20 nm and $\lambda = 0.7$ –5.6 nm, and they observed that as TB spacing decreased, the fracture strain of nanowires decreased. When the TB spacing was smaller

than 2.8 nm, dislocations nucleated inside nanowires (but near TB-surface intersections) interacted with the adjacent TBs, leading to detwinning of neighboring regions. At high stress levels, strain localization occurred in the detwinned region, which induced nanowire failure with a relatively small fracture strain (7–10%). However, when TB spacing was much larger, dislocations nucleated from the free surface and then slipped on activated slip planes within the wide twin or matrix domains. Such dislocation plasticity contributes to sample failure with large fracture strain (~30%). These behaviors are different from those observed in NT Cu nanopillars.⁹ The difference may be attributed to three factors:⁴² (1) Cu and Au have different stacking-fault energy curves and critical stress for dislocation nucleation; (2) the diameters of the investigated Cu nanopillars are approximately 2 to 12 times larger than those of the studied Au nanowires; and (3) these Au nanowires have special surface facets, different from the relatively smooth circular surfaces of the investigated Cu nanopillars.

Recently, Yuan and Wu⁴³ investigated the fracture behavior of NT Cu with hierarchically twinned structures using MD simulations on quasi-3D samples. For the simulated samples, TB spacing in the first-order twin varied from 10.44–20.87 nm, whereas the TB spacing in the second-order twin was in the range of 2.09–10.44 nm. The simulation results showed that due to the presence of second-order twins, the cracks on TBs in the first-order twins became blunt due to dislocation emission, or due to coalescence with nanovoids nucleated ahead of the crack tip, even if the cracks originally propagated via cleavage along a single TB. The results also indicated that for fixed first-order TB spacing, the fracture toughness could be improved by decreasing second-order TB spacing. A theoretical model⁴⁴ was proposed to further explain the enhancement of fracture toughness in metals with hierarchically twinned structures. The results revealed that the detwinning in the second-order twins to some extent facilitates strong crack blunting,⁴⁴ and there exists an optimized second-order TB spacing corresponding to maximum fracture toughness.⁴⁴

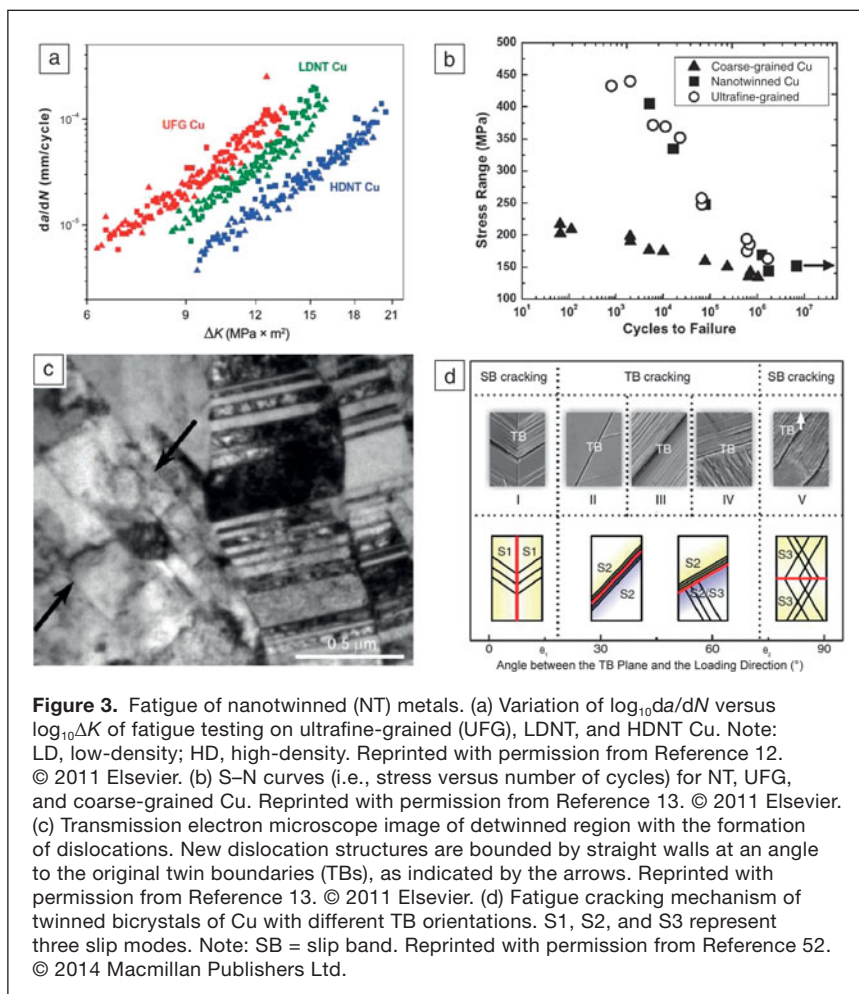
To date, a clear and comprehensive understanding of the interaction between cracks and TBs is still lacking. Recent high-resolution TEM observations in NT Ag thin films⁴⁵ revealed the detailed process of crack penetration across a twin with $\lambda = \sim 4$ nm. This process involves alternating crack-tip blunting, crack deflection, and TB migration. These deformation mechanisms are associated with the types of dislocations emitted from crack tips and the distance between crack tips and TBs. Zhou and Gao⁴⁶ performed full 3D MD simulations of dislocation interactions with TBs in front of a crack tip

in NT Cu (with $\lambda = 10$ nm). They found that the dislocation-TB interaction leads to the formation of necklace-like dislocations with unit jogs (i.e., a dislocation segment produced by interaction between two dislocation lines) on TBs. This jogged dislocation motion requires overcoming the lattice friction on unit jogs.⁴⁶ This new type of TB-related dislocation mechanism may play an important role in deformation near crack tips in NT metals.

Fatigue of nanotwinned metals

Fatigue reflects the mechanical response of materials under cyclic loading. Fatigue properties of materials are central to the design and application of materials in engineering. Limited information is available on the fatigue properties of NT metals.

Singh et al.¹² conducted the earliest study on low-cycle fatigue of a NT metal. They studied tension–tension cyclic loading of two electrodeposited NT Cu specimens with equiaxed grains (with the same mean grain size $d = 400$ – 500 nm, but $\lambda = 32$ – 85 nm) and one UFG twin-free counterpart. **Figure 3a** shows the variation of the fatigue crack growth rate da/dN , where a is the crack length and N is the number of load cycles, as a function of stress intensity amplitude ΔK from the experimental measurements.¹² This result indicates that for a fixed



grain size, the fatigue resistance of NT metals can be enhanced by increasing the twin density (i.e., decreasing TB spacing). An estimation of the crack-tip opening displacement (CTOD) versus TB spacing suggested that significantly reduced CTOD with smaller TB spacing contributes to the enhanced fatigue resistance.¹²

Shute et al.¹³ also performed tension–tension fatigue tests on magnetron sputtered NT Cu with columnar grains (with $\lambda = 35$ nm), but found that the S–N curve (i.e., stress versus number of cycles) of the NT specimen was remarkably similar to that of UFG specimens¹³ (as shown in Figure 3b). The TEM image in Figure 3c shows that some original columnar NT structures were destroyed due to detwinning during fatigue, with the formation of dislocation structures. As a result, the detwinned regions became softer compared to the neighboring twinned regions. The similarity of the S–N curves between the NT and UFG specimens is thought to arise from the crack nucleation/initiation from the boundary of the two columns and the intersection between detwinned soft regions and the free surface.

Yoo et al.⁴⁷ recently performed high-cycle fatigue experiments on magnetron sputtered 20- μm -thick columnar-grained NT Cu foils (with $\lambda = 25$ nm), where CTBs were oriented parallel to the surface. Quantitative characterization of the final twin density after fatigue-induced detwinning showed a strong coupling to the applied strain amplitude.⁴⁷ Due to the experimental setup, detwinning started near the cantilever fixture from the surface, allowing for extrusion formation and crack initiation at the surface.⁴⁷ The cracks started to extend perpendicular to the surface in a Mode I orientation, until the interaction with a CTB led to crack branching as well as diversion into a Mode II orientation,⁴⁷ disabling the cracks altogether. This is in contrast to the tension–tension experiments conducted by Shute et al.,¹² as local softening would not lead to uncontrolled detwinning followed by plastic localization and failure. Such “disabled” cracks could be found at various locations while detwinning continued below and around the cracks.⁴⁷ This hints at the possibility of disabling cracks by using CTBs to divert a Mode I crack into a Mode II configuration.

Zhou et al.⁴⁸ most recently performed a series of atomistic simulations for the cyclic deformation of NT Cu (with $d = 10$ – 20 nm and $\lambda = 0.83$ – 5.01 nm). They observed from the atomistic simulations that the fatigue cracks in NT samples advanced by alternating crack-tip blunting and resharpening due to dislocation emission and slip. This is distinct from the fatigue mechanism in the twin-free counterparts, where the fatigue crack grows by linking the nanovoids ahead of the crack tip. The simulations also revealed that detwinning dominates plastic deformation during fatigue of NT samples with a high density of twins, which is consistent with observations from the fatigue experiments.¹³

A combination of the experimental¹² and simulation results⁴⁸ indicates that as the twin density (quantified by d/λ) increases, the fatigue resistance of NT metals is substantially enhanced. Zhou et al.⁴⁸ showed that stable fatigue

crack growth conforms to Paris’s Law (i.e., a power law

$\frac{da}{dN} = C(\Delta K)^m$, where C and m are material constants) with

an exponent $m \sim 4$ by analyzing the relationship between fatigue crack growth rate da/dN and the amplitude of applied stress intensity factor ΔK from experiments and simulations. Based on the damage accumulation model, they also derived the following equation⁴⁸ in the form of Paris’s Law:

$$\frac{da}{dN} = \frac{5\pi}{96\alpha\sigma_y^2 K_{IC}^2} (\Delta K)^4, \quad (1)$$

where σ_y is the yield strength, K_{IC} is the fracture toughness under quasistatic loading, and α is a material constant (approximately 3000 for Cu). The prediction of the constant coefficient in Paris’s Law from Equation 1 is in agreement with experimental measurements.¹² Equation 1 implies that NT metals have stronger fatigue resistance because of their higher strength and fracture toughness than their twin-free counterparts.

Chowdhury et al.^{49,50} recently developed a combined atomistic and mesoscopic model to highlight the role of cyclic dislocation–TB interactions and the irreversibility of cyclic dislocation slip during fatigue crack propagation in NT metals. Based on the irreversibility of dislocation slip from crack tips during the cyclic flow, they also predicted an effective threshold of stress intensity factor range for fatigue and noted that the threshold level of short cracks was significantly affected by nanoscale twins.⁵⁰

A high density of TBs can enhance fatigue resistance, but a TB is not always strong enough to resist fatigue cracking. Some experimental observations^{51–53} showed that fatigue cracks can initiate from CTBs. Li et al.⁵² systematically investigated the cyclic deformation of Cu bicrystals with a single TB, and revealed the fatigue cracking behavior of TBs strongly depended on TB orientation with respect to the loading direction. As illustrated in Figure 3d, when the loading direction is parallel or perpendicular to the TB (Regimes I or V in Figure 3d), the fracture crack always prefers to nucleate along the slip band (SB); when the loading direction is inclined to the TB (Regimes II, III, or IV in Figure 3d), the fatigue crack first initiates from the TB. Essentially, this fatigue crack behavior is associated with the activation of different slip modes. This work provides important implications for designing engineering materials with optimized interfacial fatigue properties. It is to be noted that in the above studies,^{51–53} the TB spacing is around several microns, and sometimes even larger. If the TB spacing is reduced below 100 nm, whether the crack can still initiate from TBs during fatigue remains unknown. The fatigue properties of nanoscale twins clearly require further detailed studies, where *in situ* observations of fatigue crack initiation around nanoscale twins are key.

Creep of nanotwinned metals

In contrast to fracture and fatigue, there is much less research on the creep properties of NT metals. Bezares et al.¹⁴ performed cyclic nano- and microindentation creep measurements on NT

Cu and Ag. **Figure 4a** shows the indentation creep of electrodeposited NT Cu under a peak load of 1700 μN .¹⁴ The creep strains became saturated after tens of seconds, which is 2–3 orders of magnitude shorter than the typical creep time for nanocrystalline Cu.¹⁴ It was also found that during creep, the hardness of NT Cu (with $\lambda = 40$ nm) initially decreased and then tended to saturate after hundreds of seconds.

Figure 4b summarizes the microindentation creep results for four samples: electrodeposited NT Cu ($\lambda = 30$ nm), nanocrystalline Cu ($d = 45$ nm), magnetron sputtered NT Cu ($\lambda = 7$ nm), and Ag ($\lambda = 9$ nm). The hardness reduced over a considerable indenter dwell-time period with an approximately linear relationship between hardness and the logarithm of time. NT Cu exhibits a lower reduction rate of hardness than nanocrystalline Cu, indicating that NT metals have enhanced creep and structural stability compared to their twin-free counterparts. For nanocrystalline metals, the reduction in hardness is attributed to the rapid growth of nanosized grains.⁵⁴ However, for NT metals, the mechanisms responsible for the reduction in hardness during creep remain unknown. It should be noted in

Figure 4b that the magnetron sputtered NT Cu exhibited better stability than the electrodeposited NT Cu, due to the much thinner twin lamellae of magnetron sputtered NT Cu.

Jiao and Kulkarni⁵⁵ recently conducted a series of MD simulations for high-temperature creep in polycrystalline NT Cu (with $d = 10.3$ nm and $\lambda = 0.6$ – 5.0 nm). The simulation results showed that the creep stability significantly depended on TB spacing, and the creep strain rate had a power-law relationship with the applied stress, where the stress exponent increased from 1 to ~ 5 as the applied stress increased. It was observed that in NT samples with smaller TB spacing, TB migration due to dislocation nucleation from TB–GB intersections was a controlling mechanism during creep at high stress levels. This mechanism is distinct from the observed GB diffusion and sliding during the creep of nanocrystalline metals.

It is well known that for metals with low stacking-fault energy, continuous radiation exposure can induce noticeable void growth and swelling in materials.⁵⁶ Chen et al.⁵⁶ conducted a recent experimental study and reported that NT Cu with preexisting nanovoids could efficiently absorb radiation-induced defects (such as point defects and dislocation loops), leading to the elimination of nanovoids. This self-healing capability arises from the underlying behavior whereby networks consisting of a high density of CTBs/ITBs are able to rapidly transport the radiation-induced defects to nanovoids. This study suggests that NT metals with initial nanovoids might have good creep stability in extreme irradiation environments.

Summary

This article presented a brief survey of recent studies on the fracture, fatigue, and creep of NT metals. Experimental and computational studies have shown that NT metals exhibit remarkable fracture toughness, strong fatigue resistance, and good creep stability in comparison to their twin-free nanocrystalline or UFG counterparts. We discussed some underlying deformation mechanisms responsible for these unusual mechanical properties of NT metals, placing emphasis on the complex interactions among dislocations, cracks, and TBs.

Despite the rapid progress made in recent years, a fundamental understanding of the damage/failure process in the fracture, fatigue, and creep of NT metals is still in its infancy. There are unsolved problems that are crucial for understanding the failure of NT metals, such as (a) How do coarse/deep dimples form during fracture of NT metals?; (b) How do cracks interact with TBs during fracture or fatigue in NT metals?; (c) How do crack-TB interactions depend on TB spacing and TB orientation?;

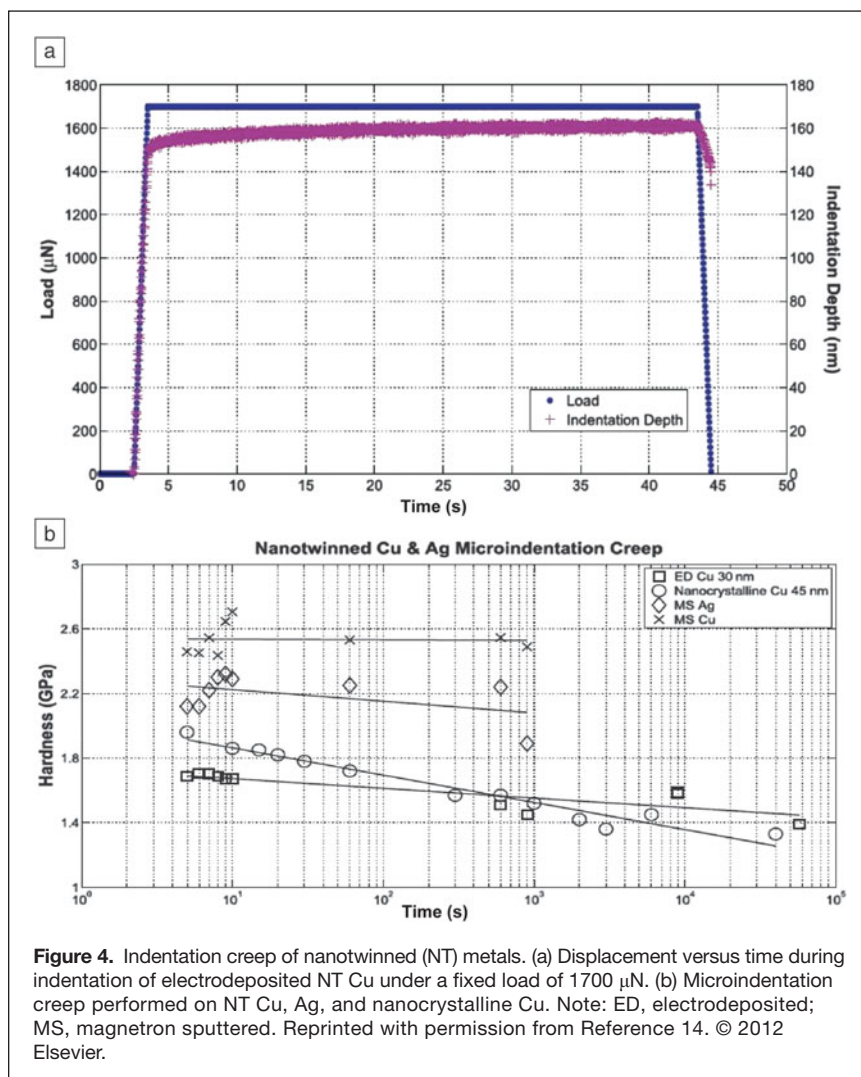


Figure 4. Indentation creep of nanotwinned (NT) metals. (a) Displacement versus time during indentation of electrodeposited NT Cu under a fixed load of 1700 μN . (b) Microindentation creep performed on NT Cu, Ag, and nanocrystalline Cu. Note: ED, electrodeposited; MS, magnetron sputtered. Reprinted with permission from Reference 14. © 2012 Elsevier.

and (d) What is the mechanism behind the hardness reduction of NT metals during indentation creep? In order to improve our understanding of, and to enhance the mechanical properties of NT materials, there is an urgent need to carry out further experimental and computational investigations on fracture, fatigue, and creep of NT metals.

Acknowledgments

X.L. and H.G. thank Ke Lu, Lei Lu, and Yujie Wei from the Chinese Academy of Sciences for stimulating discussions, and acknowledge financial support by NSF through Award CMMI-1161749 and the MRSEC Program through Award DMR-0520651 at Brown University. X.L. also acknowledges support by the NSFC Grants 11372152 and 51420105001. M.D. acknowledges support from Singapore MIT Alliance (SMA). A.M.H acknowledges NSF Award DMR-0955338.

References

1. L. Lu, Y. Shen, X. Chen, L. Qian, K. Lu, *Science* **304**, 422 (2004).
2. L. Lu, X. Chen, X. Huang, K. Lu, *Science* **323**, 607 (2009).
3. K. Lu, L. Lu, S. Suresh, *Science* **324**, 349 (2009).
4. O. Anderoglu, A. Misra, H. Wang, F. Ronning, M.F. Hundley, X. Zhang, *Appl. Phys. Lett.* **93**, 083108 (2008).
5. D. Bufford, H. Wang, X. Zhang, *Acta Mater.* **59**, 93 (2011).
6. A.M. Hodge, Y.M. Wang, T.W. Barbee Jr., *Scr. Mater.* **59**, 163 (2008).
7. H. Idrissi, B. Wang, M.S. Colla, J.P. Raskin, D. Schryvers, T. Pardoen, *Adv. Mater.* **23**, 2119 (2011).
8. D. Jang, C. Cai, J.R. Greer, *Nano Lett.* **11**, 1743 (2011).
9. D. Jang, X. Li, H. Gao, J.R. Greer, *Nat. Nanotechnol.* **12**, 4605 (2012).
10. E.W. Qin, L. Lu, N.R. Tao, J. Tan, K. Lu, *Acta Mater.* **57**, 6215 (2009).
11. E.W. Qin, L. Lu, N.R. Tao, K. Lu, *Scr. Mater.* **60**, 539 (2009).
12. A. Singh, L. Tang, M. Dao, L. Lu, S. Suresh, *Acta Mater.* **59**, 2437 (2011).
13. C.J. Shute, B.D. Myer, S. Xie, S.Y. Li, T.W. Barbee, A.M. Hodge, J.R. Weertman, *Acta Mater.* **59**, 4569 (2011).
14. J. Bezares, S. Jiao, Y. Liu, D. Bufford, L. Lu, X. Zhang, Y. Kulkarni, R.J. Asaro, *Acta Mater.* **60**, 4623 (2012).
15. H. Kou, J. Lu, Y. Li, *Adv. Mater.* **26**, 5518 (2014).
16. Y. Wei, Y. Li, L. Zhu, Y. Liu, X. Lei, G. Wang, Y. Wu, Z. Mi, J. Liu, H. Wang, H. Gao, *Nat. Commun.* **5**, 3580 (2014).
17. I.J. Beyerlein, X. Zhang, A. Misra, *Annu. Rev. Mater. Res.* **44**, 329 (2014).
18. S. Mahajan, *Scr. Mater.* **68**, 95 (2013).
19. R.J. Asaro, S. Suresh, *Acta Mater.* **53**, 3369 (2005).
20. M. Dao, L. Lu, Y.F. Shen, S. Suresh, *Acta Mater.* **54**, 5421 (2006).
21. T. Zhu, J. Li, A. Samanta, H.G. Kim, S. Suresh, *Proc. Natl. Acad. Sci. U.S.A.* **104**, 3031 (2007).
22. X. Li, Y. Wei, L. Lu, K. Lu, H. Gao, *Nature* **464**, 877 (2010).
23. A. Stukowski, K. Albe, D. Farkas, *Phys. Rev. B Condens. Matter* **82**, 224103 (2010).
24. Y. Kulkarni, R.J. Asaro, *Acta Mater.* **57**, 4835 (2009).
25. Y. Zhang, H. Huang, *Nanoscale Res. Lett.* **4**, 34 (2009).
26. C. Deng, F. Sansoz, *Nano Lett.* **9**, 1517 (2009).
27. L. Zhu, H. Ruan, X. Li, M. Dao, H. Gao, J. Lu, *Acta Mater.* **59**, 5544 (2011).
28. Z. You, X. Li, L. Gui, Q. Lu, T. Zhu, H. Gao, L. Lu, *Acta Mater.* **61**, 5217 (2013).
29. F. Yuan, X. Wu, *J. Appl. Phys.* **113**, 203516 (2013).
30. F. Yuan, P. Cheng, X. Wu, *Philos. Mag. Lett.* **94**, 514 (2014).
31. H. Zhou, X. Li, S. Qu, W. Yang, H. Gao, *Nano Lett.* **14**, 5075 (2014).
32. P. Gu, M. Dao, S. Suresh, *Acta Mater.* **67**, 409 (2014).
33. N. Lu, K. Du, L. Lu, H.Q. Ye, *Nat. Commun.* **6**, 7648 (2015).
34. T. Zhu, H.J. Gao, *Scr. Mater.* **66**, 843 (2012).
35. X. Li, H. Gao, *Nano and Cell Mechanics: Fundamentals and Frontiers*, H. Espinosa, G. Bao, Eds. (Wiley, Chichester, 2013), p. 129.
36. Y. Cheng, Z.H. Jin, Y.W. Zhang, H. Gao, *Acta Mater.* **58**, 2293 (2010).
37. M. Seita, J.P. Hanson, S. Gradecak, M.J. Demkowicz, *Nat. Commun.* **6**, 6164 (2015).
38. S. Kim, X. Li, H. Gao, S. Kumar, *Acta Mater.* **60**, 2959 (2012).
39. Z. Shan, L. Lu, A.M. Minor, E.A. Stach, S.X. Mao, *JOM* **60**, 71 (2008).
40. Z. Zeng, X. Li, L. Lu, T. Zhu, *Acta Mater.* **98**, 313 (2015).
41. A. Kobler, A.M. Hodge, H. Hahn, C. Kübel, *Appl. Phys. Lett.* **106**, 261902 (2015).
42. J. Wang, F. Sansoz, J. Huang, Y. Liu, S. Sun, Z. Zhang, S.X. Mao, *Nat. Commun.* **4**, 1742 (2013).
43. F.P. Yuan, X.L. Wu, *Philos. Mag.* **93**, 3248 (2013).
44. J. Li, Y. Ni, A.K. Soh, X.L. Wu, *Mater. Res. Lett.* **3**, 190 (2015).
45. L. Liu, J. Wang, S.K. Gong, S.X. Mao, *Sci. Rep.* **4**, 4397 (2014).
46. H. Zhou, H. Gao, *J. Appl. Mech.* **82**, 071015 (2015).
47. B.G. Yoo, S.T. Bolesb, Y. Liu, X. Zhang, R. Schwaiger, C. Eberl, O. Kraft, *Acta Mater.* **81**, 184 (2014).
48. X. Zhou, X. Li, C. Chen, *Acta Mater.* **99**, 77 (2015).
49. P.B. Chowdhury, H. Sehitoglu, R.G. Rateick, *Int. J. Fatigue* **68**, 277 (2014).
50. P.B. Chowdhury, H. Sehitoglu, R.G. Rateick, *Int. J. Fatigue* **68**, 292 (2014).
51. S. Qu, P. Zhang, S.D. Wu, Q.S. Zang, Z.F. Zhang, *Scr. Mater.* **59**, 1131 (2008).
52. L.L. Li, Z.J. Zhang, P. Zhang, Z.G. Wang, Z.F. Zhang, *Nat. Commun.* **5**, 3536 (2014).
53. C.A. Stein, A. Cerrone, T. Ozturka, S. Lee, P. Kenesei, H. Tucker, R. Pokharel, J. Lind, C. Hefferan, R.M. Suter, A.R. Ingraffea, A.D. Rollett, *Curr. Opin. Solid State Mater. Sci.* **18**, 244 (2014).
54. K. Zhang, J.R. Weertman, J.A. Eastman, *Appl. Phys. Lett.* **85**, 5197 (2004).
55. S. Jiao, Y. Kulkarni, *Comput. Mater. Sci.* **110**, 254 (2015).
56. Y. Chen, K.Y. Yu, Y. Liu, S. Shao, H. Wang, M.A. Kirk, J. Wang, X. Zhang, *Nat. Commun.* **6**, 7036 (2015). □

SOCIETY NEWS | UPCOMING MEETINGS

International Conference on Optics, Photonics and Materials to be held in France www.nice-optics2016.com

The 1st International Conference on Optics, Photonics and Materials will be held October 26–28 in Nice, France.

The conference will cover emerging fields in optics, materials sciences, physics, and biology in four main themes. Nonlinear Optics and Complex Dynamics will cover topics such as nonlinear beams, optical vortices, and disorder and nonlinearity; Soft Matter Materials will cover topics such as liquid-crystal optics and technologies, colloidal interface, and nanoparticles interface;

Optical Metrology will cover topics such as adaptive optics, microscopy, and ultrafast optical phenomena; and Biophotonics & Biosensors will cover topics such as imaging in scattering media, photo-acoustics, and optical coherence tomography. Scientists can use their knowledge of these fields to engineer new artificial materials, systems, and devices for applications in the medical, industrial, military, and energy sectors.

Plenary speakers are Pablo Artal of the University of Murcia, Spain; Robert

W. Boyd of the University of Rochester, USA; Giulio Cerullo of Polytechnic University of Milan, Italy; and Demetri Psaltis of École Polytechnique Fédérale de Lausanne, Switzerland. There will also be a number of keynote speakers.

The submission deadline is April 30. The notification deadline is May 15. Early bird registration ends June 15. More information can be accessed from the conference website at www.nice-optics2016.com or by email at contact@nice-optics2016.com.